Hydrogen-effusion-induced structural changes and defects in *a*-Si:H films: Dependence upon the film microstructure

K. Zellama
Laboratoire de Physique des Couches Minces, Faculté des Sciences d'Amiens, 33 rue Saint Leu, 80039 Amiens, France, and Groupe de Physique des Solides, URA CNRS 17, Université Paris VII, 2 place Jussieu, 75251 Paris Cédex 05, France

L. Chahed,* P. Sládek,† and M. L. Thèye
Laboratoire d'Optique des Solides, URA CNRS 781, Université Pierre et Marie Curie, 4 place Jussieu, 75252 Paris Cédex 05, France

J. H. von Bardeleben
Groupe de Physique des Solides, URA CNRS 17, Université Paris VII, 2 place Jussieu, 75251 Paris Cédex 05, France

P. Roca i Cabarrocas
Laboratoire de Physique des Interfaces et des Couches Minces, UPR CNRS 258, Ecole Polytechnique, 91128 Palaiseau Cédex, France
(Received 3 February 1995; revised manuscript received 17 October 1995)

In order to better understand the effects of hydrogen incorporation and departure on the defects and the disorder in undoped hydrogenated amorphous silicon (*a*-Si:H), we performed a comparative study on samples deposited under different plasma conditions. We used a combination of IR absorption spectroscopy, electron-spin resonance, photothermal deflection spectroscopy, constant photocurrent method, and elastic recoil detection analysis measurements to determine the changes in the defect density and in the disorder, as well as in the hydrogen concentration and bonding modes, after isochronal annealing cycles at temperatures up to 500–600 °C. The results, which show a better stability of the bonded hydrogen in the films deposited at high rates, are interpreted as a whole in terms of specific local hydrogen bonding environments, related to different growth mechanisms.

I. INTRODUCTION

The hydrogen atoms incorporated in the *a*-Si:H samples during deposition not only saturate silicon dangling bonds, which leads to a decrease of the density of defect states in the gap, but also reduce the structural disorder, which results in a narrowing of the band tails. Consequently, hydrogen is of crucial importance for the improvement of the electronic and optical properties of *a*-Si:H.[1] It has also been clearly established that the defect state density and the disorder depend on both the amount and the bonding configurations of hydrogen in the samples, which are in turn deeply dependent on the deposition conditions. Great efforts have been dedicated to the optimization of the deposition parameters in order to produce *a*-Si:H samples with low defect density ($\leqslant 10^{16}$ cm^{-3}).[2–5] This is achieved for deposition temperatures ranging from 150 to 300 °C under the so-called optimized ''standard'' plasma conditions: pure silane, low rf power (10 mW/cm^2), low gas pressure (3–10 Pa), and low deposition rates ($\sim$1 Å/s), also referred to as chemical-vapor-deposition- like conditions. However, the low deposition rates and the high compressive stress in the films make it difficult to grow thick layers. To overcome these difficulties we have developed a new process in which *a*-Si:H is deposited from the dissociation of silane and helium mixtures at high rf power (85 mW/cm^2), high pressure (75 Pa), and high depositions rates (8–30 Å/s).[6–8] The studies conducted so far on the films deposited from silane-helium mixtures, referred to as ''He-diluted'' samples in the following, have shown that, under certain deposition conditions, the bonded hydrogen distribution and the microstructure in these samples are very different from those in the ''standard'' samples.[9,10]

In order to obtain more information about these differences, we performed a comparative investigation of the effects of isochronal annealing cycles at increasing temperatures on the hydrogen bonding and the electronic properties of ''standard'' and He-diluted *a*-Si:H samples using several complementary measurements such as infrared absorption (IR), elastic recoil detection analysis (ERDA), electron-spin resonance (ESR), photothermal deflection spectroscopy (PDS), and photoconductivity by the constant photocurrent method (CPM). We paid special attention to the positions and the relative amplitudes of the IR features currently attributed to Si-H, Si-H_2, and (Si-H_2)$_n$ groups in the wagging, bending, and stretching vibrational absorption bands.

II. EXPERIMENT

Four types (1–4) of undoped *a*-Si:H films were deposited by the plasma enhanced chemical vapor decomposition (PECVD) of either pure silane (types 1–3) or a mixture of 40% silane in helium (type 4). The preparation conditions are summarized in Table I. We stress that the samples selected here are representative of each type of film. The types 1–3 films, deposited under ''standard'' plasma conditions, differ by the value of the substrate temperature during deposition. The type 3 film deposited at 250 °C corresponds to the optimized *a*-Si:H. The type 4 film, deposited under different plasma conditions leading to high deposition rates, is intentionally deposited at the same temperature as the type 3 film.

 © 1996 The American Physical Society

TABLE I. Deposition conditions of the a-Si:H films of types 1–4. Types 1–3 films are deposited from pure silane while type 4 films are obtained from the dissociation of a mixture of 40% silane in He. The total bonded H concentration C_H as well as the optical gap E_{04} are also reported.

Type of film	Ref. sample	T_s (°C)	P (Pa)	rf (W)	d (μm)	r_d (Å/s)	E_{04} (eV)	C_H (at. %)
1	207101	50	6	2	0.95	0.45	1.94	23
2	207092	100	6	2	1.40	0.50	1.95	15
3	807221	250	6	0.5	4.46	0.80	1.89	10
4	207035	250	73	12	3.45	8.0	1.92	13

The hydrogen content and bonding configurations are deduced from IR absorption measurements. The IR spectra are obtained at room temperature using a Bomem DA 3.01 Fourier transform spectrometer in the 450–3500 cm^{-1}, with a resolution of 2 cm^{-1}, by averaging up to 2000 scans in order to improve the signal-to-noise ratio. Using the proportionality constants previously reported,[11] $A_{640}=2.1\times10^{19}$ cm^{-2}, $A_{2000}=9\times10^{19}$ cm^{-2}, $A_{2080}=2.21\times10^{20}$ cm^{-2}, we can estimate (i) the total content of the bonded hydrogen C_H from the wagging band around 640 cm^{-1}, (ii) the concentration

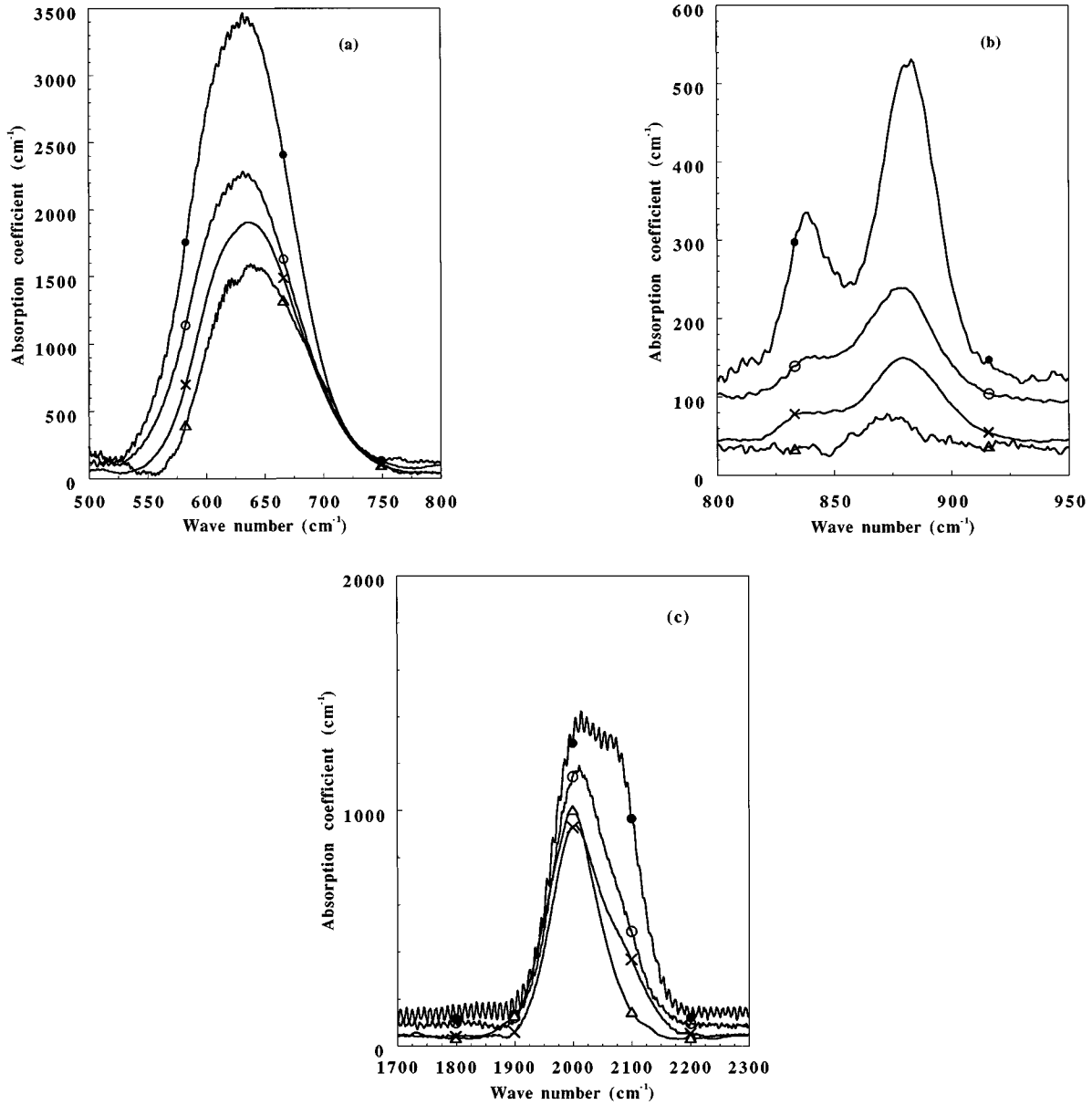

FIG. 1. Typical IR absorption spectra obtained for the types 1–4 films in the as-deposited state: ●, type 1; ○, type 2; △, type 3; and ×, type 4, for the different absorption modes [(a) wagging mode, (b) bending mode, and (c) stretching mode].

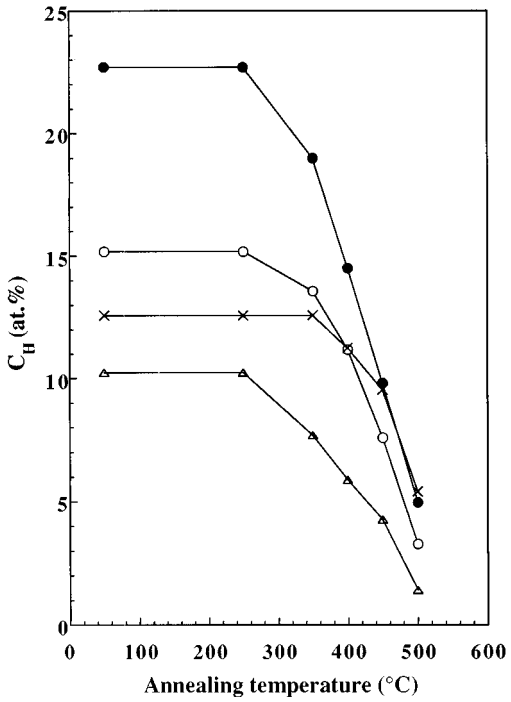

FIG. 2. Variation of the total bonded hydrogen content C_H (630–640-cm^{-1} band) as a function of the annealing temperature for the types 1–4 films: ●, type 1; ○, type 2; △, type 3; and ×, type 4.

C_{H1} of hydrogen bonded as isolated monohydride groups (Si-H) contributing to the 2000-cm^{-1} stretching band, (iii) the concentration C_{H2} of the polyhydride (SiH_x) and/or clustered monohydride $(SiH)_x$ groups that contribute to the 2080-cm^{-1} stretching band.

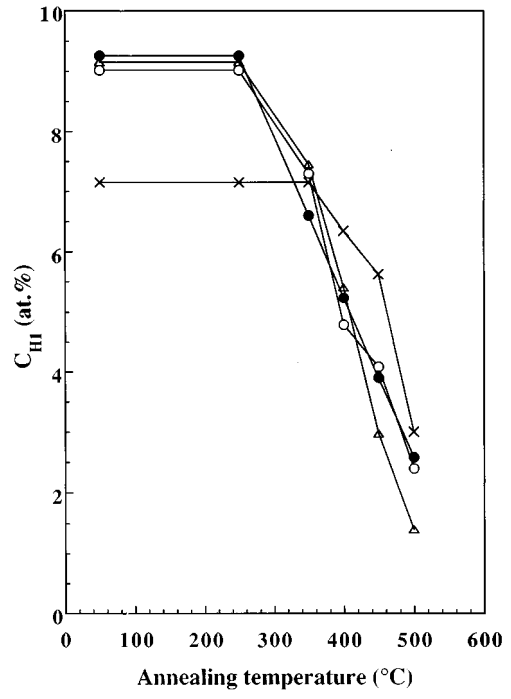

FIG. 3. Variation of the concentration C_{H1} of hydrogen bonded as isolated monohydride groups (2000 cm^{-1}) as a function of the annealing temperature for the types 1–4 films: ●, type 1; ○, type 2; △, type 3; and ×, type 4.

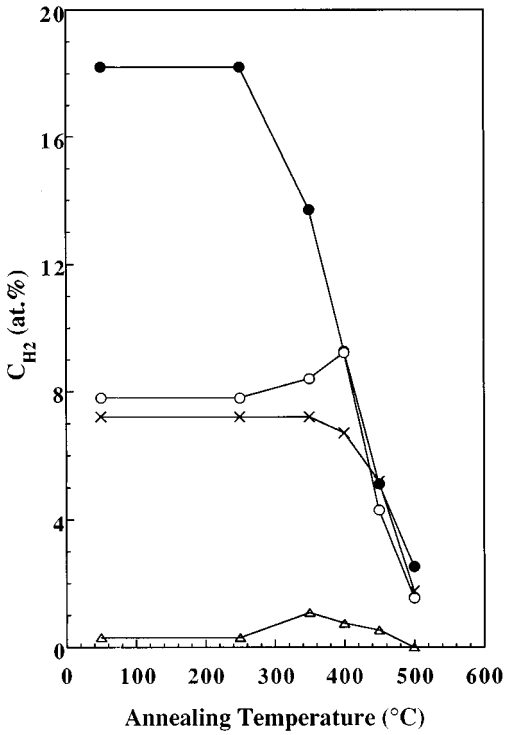

FIG. 4. Variation of the concentration C_{H2} of hydrogen bonded as polyhydride groups or Si-H groups in cavities (2080 cm^{-1}) as a function of the annealing temperature for the types 1–4 films: ●, type 1; ○, type 2; △, type 3; and ×, type 4.

We also determined the microstructure parameter R[8] defined as the ratio of the integrated intensity of the 2080–2100 cm^{-1} band over the total integrated intensity of the stretching (2000 and 2080–2100 cm^{-1}) band, $R=[2080]/([2000]+[2080])$, and we considered the integrated intensities of the two components of the bending bands at 840 and 880 cm^{-1}, which give information about the amount of $(Si\text{-}H_2)_n$ chains that may be present in the samples.

ERDA experiments were also performed to determine the total hydrogen concentration in types 3 and 4 films.

Combined optical transmission, PDS, and CPM measurements allow the determination of the optical gap E_{04}, of the disorder parameter E_0, and of the ''optical'' deep defect density N_D. We focus here on the values of E_0 and N_D obtained from the analysis of the calibrated CPM-derived optical absorption spectra down to 0.6 eV. The method and the model used for this analysis are presented in detail in a previous paper;[12] the model-dependent uncertainty for the determination of N_D is less than 50%. The values of N_D are compared with those of the neutral dangling bond density N_S obtained from ESR experiments and corresponding to $g=2.0055$. The detection limit is of the order of 10^{16} cm^{-3}. The estimated uncertainty in the determination of the absolute values of N_s is of the order of 50%. Errors on the relative measurements are, however, lower than 10% for both N_D and N_S.

All these measurements are carried out on the types 1–4 films in their as-deposited state and after successive annealing steps at increasing temperature T_A from 250 to 500–

TABLE II. Values of the microstructure parameter R and of the integrated intensities of the 840- and 880-cm^{-1} IR bending modes as a function of the annealing temperature T_A for the films 1–4.

Type of film	Parameter	As-deposited	250 °C	350 °C	400 °C	450 °C	500 °C
	R	0.45	0.45	0.46	0.43	0.39	0.29
1	[840] cm^{-2}	5070	5070	3120	1400	0	0
	[880] cm^{-2}	12190	12190	8610	4760	1970	0
	R	0.26	0.26	0.33	0.45	0.3	0.23
2	[840] cm^{-2}	1310	1310		0	100	0
	[880] cm^{-2}	5040	5040		3110	1130	0
	R	0.03	0.03	0.11	0.1	0	0
3	[840] cm^{-2}	0	0	0	0	0	0
	[880] cm^{-2}	0	0	0	0	0	0
	R	0.29	0.29	0.29	0.31	0.28	0.17
4	[840] cm^{-2}	860	860	860	0	0	0
	[880] cm^{-2}	4020	4020	4020	2360	3140	300

600 °C for periods of 30 min. The annealing cycles are performed in a quartz tube evacuated to 10^{-8} Torr, using very low heating and cooling rates (0.5 °C/min) to avoid any quenching effects.

III. RESULTS AND DISCUSSION

A. Hydrogen bonding

The IR absorption spectra presented in Figs. 1(a), 1(b), and 1(c) show the different hydrogen bonding configurations for types 1–4 films in their as-deposited state. The intensity of the wagging band [Fig. 1(a)] around 630–640 cm^{-1} decreases as T_s increases, whatever the plasma conditions. This band shifts to higher wave numbers and its half-width decreases as T_s increases. The fit of this absorption band by a single Gaussian indicates that the wagging modes are centered around 630 cm^{-1} for types 1 and 2 films (low T_s) and around 640 cm^{-1} for types 3 and 4 films (high T_s).

Types 1, 2, and 4 films have qualitatively similar bending bands [Fig. 1(b)] with two well-separated components centered at 840 and 880 cm^{-1}, respectively. Bending bands are on the contrary hardly detectable in type 3 film, a feature currently associated to device-quality material. Types 2 and 4 films differ from type 1 film in that the 880-cm^{-1} mode is more intense than the 840-cm^{-1} one; in addition, the 840-cm^{-1} band is more pronounced for film 2 than for film 4. Type 1 film exhibits a well-defined doublet with intense bands at 840 and 880 cm^{-1}.

The stretching absorption bands [Fig. 1(c)] can be decomposed into two Gaussian components centered at 2000 and 2080 cm^{-1}, except for the type 3 film, which shows essentially a single stretching component at 2000 cm^{-1}.

The bonded hydrogen concentrations deduced from the analysis of the IR spectra, i.e., the total bonded hydrogen content C_H, the concentration C_{H1} of the hydrogen bonded as isolated monohydride groups and the concentration C_{H2} of the hydrogen bonded as polyhydrides Si-H_2, (Si-H_2)$_n$ groups and/or interacting monohydride groups are reported in Figs. 2, 3, and 4, respectively, as a function of the annealing temperature T_A.

Surprisingly enough, Fig. 3 shows that all the standard (1–3) films in their as-deposited state exhibit almost the same content of hydrogen incorporated as isolated monohydride groups (C_{H1}). Consequently, in the as-deposited state, the increase of the total bonded H concentration (C_H) as T_s decreases (Fig. 2) is essentially due to the higher amount of H incorporated as polyhydride groups and/or interacting monohydride complexes (C_{H2}), as shown in Fig. 4. As for the He-diluted type 4 film deposited at $T_s = 250$°C, it has a lower C_{H1} value than all the standard films (1–3), while its C_{H2} value is much higher than that of film 3 deposited at the same T_s, but comparable to that of film 2 deposited at 100 °C. These results indicate that the modes of H incorporation depend on both the plasma conditions and the substrate temperature.

The proportion of polyhydride complexes (Si-H_2) and/or Si-H groups in cavities is usually characterized by the so-called microstructure parameter R, the values of which are reported in Table II for films 1–4. For the standard films 1–3 in the as-deposited state, R is maximum for film 1 ($T_s = 50$ °C), decreases with increasing T_s and almost vanishes for film 3 ($T_s = 250$ °C). Furthermore, for films 1 and 2, the presence of a shoulder at 2080 cm^{-1} in the stretching band is systematically accompanied by a well-resolved doublet at 840–880 cm^{-1} in the bending mode region, which is, however, much more intense for film 1 as already emphasized [Figs. 1(b) and 1(c)]. This confirms that on the one hand, Si-H_2 and (Si:H_2)$_n$ complexes are present in these samples in addition to the monohydride groups, and that on the other hand, film 1 has a larger amount of Si-H_2 complexes as well as polymerized (Si:H_2)$_n$ groups. This is well illustrated by the behavior of the integrated intensities of the 840- and 880-cm^{-1} bands with respect to T_s presented in Table II for these films. On the contrary, in the standard film 3 the hydrogen is essentially incorporated as isolated monohydride groups. A surprising result is obtained for film 4 deposited at 250 °C. It exhibits in the as-deposited state a significantly higher total bonded hydrogen content C_H than film 3 deposited at the same T_s but under different plasma conditions (Fig. 2). Moreover, type 4 films have a large value of R as compared to $R \approx 0$ for type 3 films, and a doublet at

840–880 cm^{-1} in the bending region accompanying [Fig. 1(b)] a 2080 cm^{-1} stretching band, very similar to the features observed in the standard type 2 films deposited at much lower T_s. However, the similarities between films 2 and 4 have to be weighted by the intensity of the bending bands. As shown in Table II, the integrated intensity of the 840-cm^{-1} component is lower in type 4 than in type 2 films. This can be understood as a result of the different microstructures of these films. Indeed, growth studies[13,14] indicate that when depositing at high rates from silane-helium mixtures, there is a modification of the hydrogen incorporation in the films, attributed to the change in the nature of the film precursors. This is supported by small-angle x-ray scattering measurements,[15] which show that type 4 films have a larger void fraction than type 3 films but that the voids have similar size and shape. Therefore, even though the type 4 films have about the same microstructure parameter R as the type 2 films, their local microstructure is of a different nature because of their particular deposition conditions. This difference in the film microstructure will be one of the key factors to understand the changes of the film properties during the annealing experiments.

The variations of the H concentrations C_H, C_{H1}, and C_{H2} with the annealing temperature T_A are summarized in Figs. 2–4. It is first interesting to note that the concentrations C_H and C_{H1} start to decrease as early as $T_A = 350$ °C for all the standard types 1–3 films, while the decrease of these quantities occurs at higher temperature (400 °C) and is slower for the He-diluted type 4 films. This significant behavior already suggests that the bonded H is thermally more stable in the latter, as previously reported.[9,10] On the other hand, although the concentration C_{H1} of isolated monohydride groups decreases in a similar way for all the standard samples (Fig. 3), the concentration C_{H2} of polyhydride groups and/or clustered Si-H groups behaves differently upon annealing in type 1 and type 2 films (Fig. 4). For film 1 C_{H2} starts to decrease steadily at $T_A = 350$ °C, while for film 2 it stays almost constant, and even increases slightly up to 400 °C, then drops for higher T_A. We attribute this discrepancy to different film structure. Indeed, since type 1 films have a columnar structure and a large R value, the hydrogen released by the dissociation of the polyhydride groups can readily diffuse out of the sample, which explains the observed early decrease of C_{H2} (Fig. 4). On the contrary, type 2 films correspond to a rather dense a-Si:H material containing spherical voids. In this case, a fraction of the hydrogen released at low temperature from the dissociation of the polyhydride groups can be trapped in these cavities and possibly passivate silicon dangling bonds at their internal surfaces. The accumulation of bonded hydrogen in the cavities could then be the reason for the observed increase of C_{H2} between 250 and 400 °C. The same explanation should hold for the increase of C_{H2} detected for $T_A \approx 350$ °C in type 3 films (Fig. 4), although the void fraction is smaller than in type 2 films.

For type 4 film C_{H2} exhibits a slightly different behavior: we did not observe any increase in C_{H2} in the temperature range 350–400 °C. It remains almost constant and then drops rapidly at higher T_A. This is consistent with two facts.

(i) In type 4 film the hydrogen fraction released from isolated monohydride groups after annealing at $T_A = 400$ °C and which might contribute to the increase in C_{H2} as explained for films 2 and 3 is much smaller than in these samples (Fig. 3).

(ii) The 2080-cm^{-1} component of the stretching band in the as-deposited state must be ascribed, at least in part, to interacting SiH groups located at the internal surface of voids isolated from each other. Therefore little changes in C_{H2} are expected from these groups until high annealing temperatures. It has indeed been reported[16] that in silicon films with high void fractions, there is a delay in the hydrogen departure, as observed in our type 4 films.

We can make at this stage the following remarks.

(a) In spite of differences in the microstructure and hydrogen bonding between type 2 and type 4 films, the behavior of the hydrogen incorporated as polyhydride and/or interacting monohydride groups in these films with respect to the annealing presents some similarities. In both cases, the stretching bands still exhibit a small but non-negligible 2080-cm^{-1} component at $T_A = 500$ °C, in addition to a more pronounced 2000-cm^{-1} component (see Fig. 4 and R in Table II), while the 840-cm^{-1} component of the bending band almost vanishes at $T_A = 400$ °C. This indicates that essentially SiH_2 groups for film 2 and interacting monohydride ones for film 4 are still present in these samples after high-temperature annealing in addition to the isolated monohydride groups. On the contrary, for film 1, the 840-cm^{-1} component vanishes at $T_A = 450$ °C only, indicating the persistence in this film of some proportion of $(SiH_2)_n$ chains at higher T_A than in films 2 and 4.

(b) The decrease of C_{H1} for annealing temperatures as low as 350 °C in the standard types 1, 2, and 3 films is surprising since H incorporated as isolated monohydride groups is usually considered as ''tightly bonded'' and responsible for the ''high-temperature peak'' of the H evolution spectra.[17,18] The fact that for type 2 film C_{H1} starts to decrease at lower T_A than C_{H2} is also difficult to reconcile with commonly admitted ideas, and rather suggests a redistribution in the hydrogen bonding configurations, as indicated above.

(c) We observe in the standard type (1–3) films that annealing at T_A higher than 350 °C induces a slight shift of all the absorption bands towards lower frequencies, while the positions of these bands remain almost unchanged up to 450 °C in the He-diluted type 4 film. This confirms that the environment of the remaining Si-H bonds is less perturbed by the departure of H in the latter case.

(d) Finally, it is worth noticing that the total bonded H concentration C_H deduced from the IR absorption spectra and the total H content obtained from the ERDA measurements behave in a similar way upon annealing for types 3 and 4 films.

B. Disorder and defects

Let us now present the results from the point of view of the optoelectronic properties. Table I and Fig. 5 show that, in the as-deposited state, the optical gap E_{04} deduced from the optical absorption experiments scales, as expected, with the total bonded H content for type 2 to 4 films, whatever the modes of H incorporation. Nevertheless, E_{04} does not increase further for C_H higher than 15 at. %, as it is observed

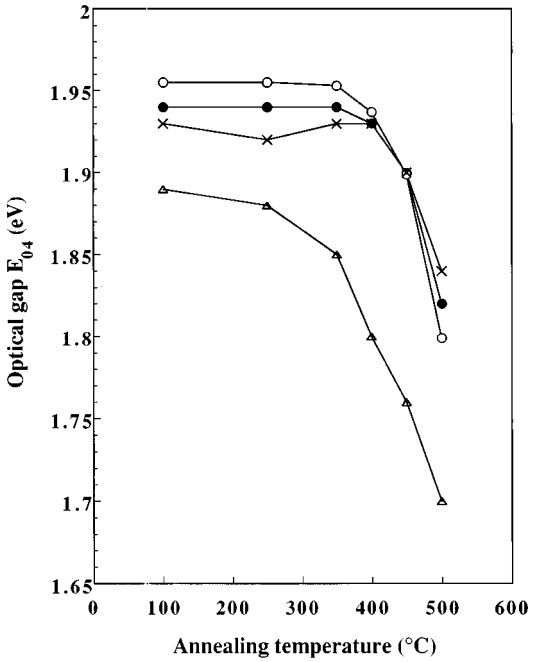

FIG. 5. Variation of the optical gap E_{04} as a function of the annealing temperature for the types 1 to 4 films: ●, type 1; ○, type 2; △, type 3; and ×, type 4.

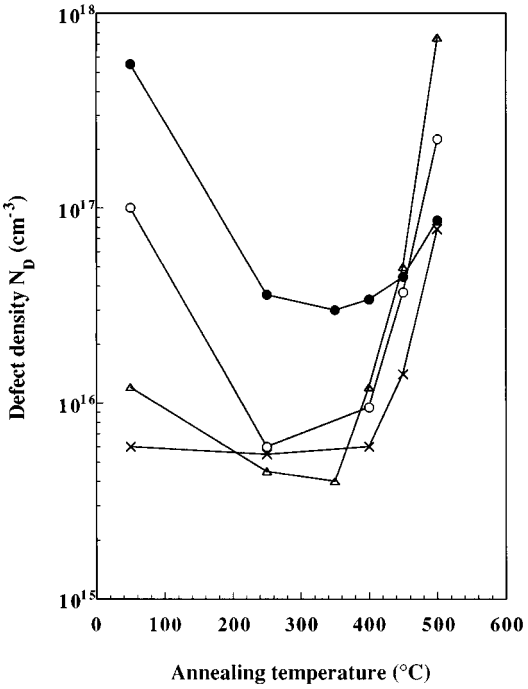

FIG. 6. Variation of the optical defect density N_D as a function of the annealing temperature for the types 1–4 films: ●, type 1; ○, type 2; △, type 3; and ×, type 4. N_D is obtained from the CPM and the PDS experiments for films 2, 3, 4, and 1, respectively.

for film 1 ($C_H = 23$ at. %). It seems therefore that the alloying effect of hydrogen incorporation saturates for $C_H \approx 15\%$ in PECVD *a*-Si:H films. Upon annealing, E_{04} decreases as T_A increases for all films, in agreement with previous reports.[19,20] However, while E_{04} starts to decrease at $T_A = 350$ °C, in agreement with the decrease of C_H, for type 3 films that contain essentially isolated monohydride groups, it stays almost unchanged up to 350 °C for types 1 and 2 films and up to 400 °C for type 4 films, i.e., up to temperatures at which C_H has already decreased. The relationship between the optical gap and the hydrogen incorporation is therefore more complex in these cases. This will be the subject of a forthcoming paper.

We turn now to the variations upon annealing of the optical defect density N_D and of the disorder parameter E_0 as deduced from the PDS and CPM experiments, and of the density of neutral dangling bonds N_s as obtained from the ESR experiments, which are reported in Figs. 6, 7, and 8, respectively. It is important to point out that for film 1 the values of N_D and E_0 are estimated from the PDS-derived optical absorption spectra only, since no photoconductivity could be measured in this film. Moreover, for types 3 and 4 films in their as-deposited state, as well as for types 2, 3, and 4 films after annealing at 250 °C, no N_s value could be obtained because the spin density was lower than the detection limit of the ESR experiments ($\approx 10^{16}$ cm^{-3}). In addition, we note that the absolute values derived for N_s are systematically larger than the corresponding N_D values by about a factor of 4 (even more for type 1 film), which can be related to the experimental uncertainties in both cases. Nevertheless N_D and N_S behave in a similar way upon annealing.

As expected, the standard types 1 and 2 films deposited at low T_s(50 and 100 °C, respectively) exhibit in the as-deposited state higher defect densities N_D (5.5×10^{17} and

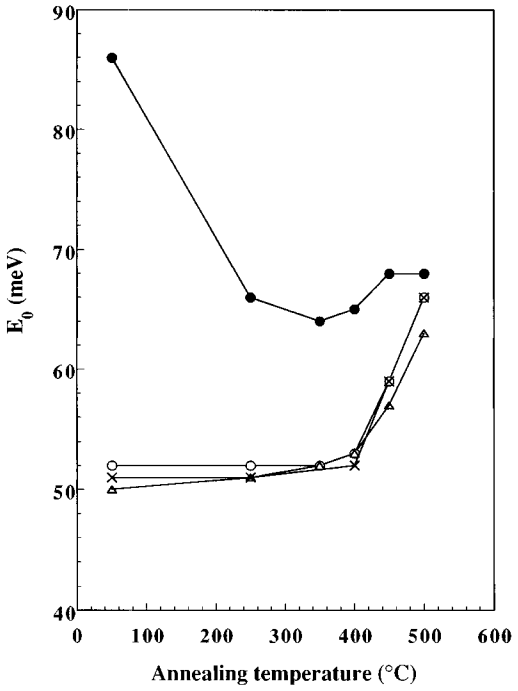

FIG. 7. Variation of the disorder parameter E_0 as a function of the annealing temperature for the types 1–4 films: ●, type 1; ○, type 2; △, type 3; and ×, type 4. For film 1, E_0 is obtained from the PDS measurements.

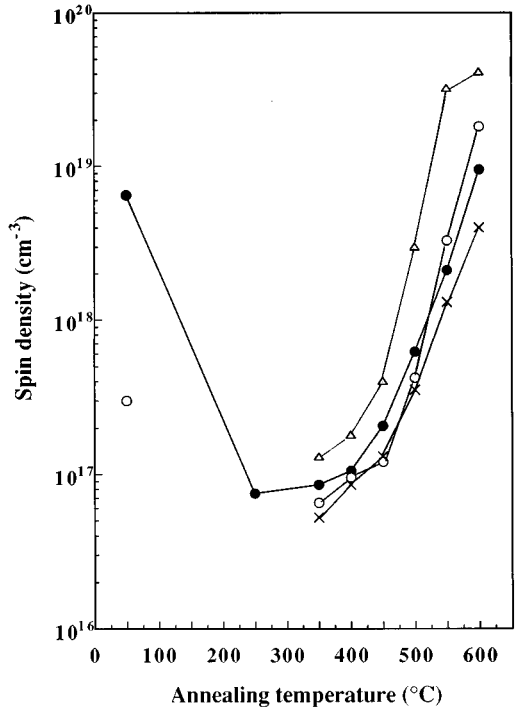

FIG. 8. Variation of the density of neutral dangling bonds N_s determined from ESR measurements as a function of the annealing temperature for the types 1–4 films: ●, type 1; ○, type 2; △, type 3; and ×, type 4. For types 3 and 4 films in the as-deposited state as well as for types 2, 3, and 4 films after annealing at 250 °C, no spin density could be measured because N_s was lower than the detection limit of the ESR experiments ($\approx 10^{16}$ cm^{-3}).

1×10^{17} cm^{-3}, respectively) than the standard type 3 film deposited at high T_s (250 °C) which has $N_D=1.2\times10^{16}$ cm^{-3} (Fig. 6). As for the disorder parameter E_0, it is about the same for types 2 and 3 films (around 51 and 50 meV, respectively) but much larger for the type 1 film (around 86 meV). This result reveals a significant difference between the two low T_S standard films. Indeed, type 2 film deposited at 100 °C contains a large defect density in its as-deposited state, like type 1 film deposited at 50 °C, but it is much less disordered; in fact, the disorder of the silicon network is comparable to that in type 3 films deposited at 250 °C.

Quite interesting results are obtained for the He-diluted type 4 film deposited at 250 °C. Although this film has a larger C_{H} than the standard type 3 film, deposited at the same T_S, and also differs from this film by its large microstructure parameter, it exhibits in its as-deposited state comparatively low defect density ($N_D=6\times10^{15}$ cm^{-3}) and disorder parameter ($E_0=51$ meV) values. This result disagrees with the accepted ideas that the presence of polyhydride complexes, giving rise to the 2080-cm^{-1} component of the stretching band, is associated with poor quality material from the point of view of its defect density.[21,22] The same conclusions can be drawn from the values of the neutral dangling bond density N_s (Fig. 8). In the as-deposited state N_s takes much higher values for films 1 and 2 (6.5×10^{18} and 3×10^{17} cm^{-3}, respectively) than for films 3 and 4 (N_s lower than 10^{16} cm^{-3}, i.e., below the detection limit of the ESR spectrometer). This study therefore confirms that the optimized type 3 and 4 films, deposited at the same T_S but under completely different plasma conditions (see Table I), have in the as-deposited state very similar defect densities although they differ by their hydrogen incorporation and their microstructure. We have recently shown that the difference in the hydrogen incorporation, however, affects the electron transport properties.[23]

Annealing at $T_A=250$ °C has practically no influence on the N_D and E_0 values for type 3 and 4 films optimized during deposition. The slight N_D decrease observed for the standard type 3 films is probably related to surface effects resulting in an enhancement of the PDS and CPM derived absorption coefficient values in the sub-band-gap region; these surface effects may be reduced by low-temperature annealing. On the contrary, annealing at $T_A=250$ °C produces a large decrease of both N_D and N_S for types 1 and 2 films, as previously reported.[8,24] This corresponds to the elimination of part of the native defects that remain in these nonoptimized standard films in their as-deposited state. There are, however, two significant differences between types 1 and 2 films. On the one hand, the N_D and N_S values remain quite high for type 1 films, while for type 2 films they become comparable to those found for the optimized types 3 and 4 films. On the other hand, for type 1 films deposited at 50 °C, the decrease of N_D and N_S is accompanied by a decrease of the disorder parameter E_0 (from 86 to 65 meV), which is in agreement with commonly admitted models[25] based on an equilibrium between weak bonds (disorder) and dangling bonds (defects). On the contrary, for film 2 deposited at 100 °C, there is no variation of E_0, which is already quite small in the as-deposited state; this suggests that under such deposition conditions there is no correlation between the silicon network, which has reached equilibrium during deposition, and the "excess" defects that are easily eliminated by low-temperature annealing.

If we now consider the effects of annealing at higher T_A for films 2 to 4, it is important to point out that no significant increase in the defect density N_D (Fig. 6) and the disorder parameter E_0 (Fig. 7) can be observed up to $T_A=350$ °C for all films, although the total bonded H content C_{H} already started to decrease above 250 °C in the standard types 1 to 3 films. However, the neutral dangling bond density N_s behaves differently. Indeed, while N_s was below the detection limit of the ESR experiments for films 2–4 for T_A between 250 and 300 °C ($N_s<10^{16}$ C m^{-3}), it increases abruptly at $T_A=350$ °C by about one order of magnitude (N_s around 1×10^{17} C m^{-3}) in all cases (Fig. 8). The starting temperature for the increase in the defect density is then lower for N_s than for N_D. This discrepancy can be tentatively explained by changes in the charge state of the dangling bond centers[26] and/or a shift of the Fermi level upon annealing. It could also be due to the presence of outdiffusion profiles that might affect differently the CPM and ESR experimental results.

For T_A higher than 400 °C, both N_D and N_s exhibit a rapid increase for all films (up to 500 °C for N_D, to 600 °C for N_s); the disorder parameter E_0 behaves in the same way. This corresponds to the creation of new defects due to the release of hydrogen from the different Si-H bonds.

As for the type 1 films that represent typical poor quality material, with high defect density and high disorder in the

as-deposited state as well as after annealing at $T_A = 250\,^{\circ}\mathrm{C}$, they are comparatively less perturbed by high-temperature annealing, at least if we consider N_D and E_0 only; indeed N_s increases with increasing T_A almost as rapidly as in types 2 to 4 films.

It is interesting to notice that the largest values of both N_D and N_s after high-temperature annealing are observed for the optimized standard type 3 film, which has in the as-deposited state the lowest total bonded hydrogen concentration C_{H}, essentially incorporated as isolated monohydride groups. The C_{H1} value in this film drops from 9.2 at. % before annealing to 1.4 at. % after annealing at 500 °C (Figs. 2–4). On the contrary, the optimized He-diluted type 4 film, which exhibits in the as-deposited state the lowest C_{H1} value but a higher total bonded H concentration C_{H}, has the lowest N_D and N_s values after high-temperature annealing. At $T_A = 500\,^{\circ}\mathrm{C}$ the values of C_{H1} and C_{H2} are, respectively, equal to about 3 at. % (significantly higher than that obtained for film 3) and 1.5 at. %. However, we observe a slightly larger disorder parameter E_0 after high-temperature annealing for film 4 than for film 3. Film 2 lies between film 3 and film 4 from the point of view of the changes in N_D and N_S for T_A higher than 350 °C.

If we consider the experimental results as a whole, they indicate that the defect creation process upon annealing, (i.e., release of the hydrogen from the different Si-H bonds) seems to be essentially governed by the particular film microstructure resulting from the deposition conditions. However, the concentration of the isolated monohydride groups initially present in the films seems also to play an important role in this process. In addition, although the He-diluted type 4 film deposited at high rate contains, at least in the as-deposited state, an important proportion of clustered Si-H groups and a certain amount of H incorporated as polyhydride complexes, it shows more hydrogen stability with respect to annealing than the standard films deposited at low rates, especially type 3 film deposited at the same $T_S = 250\,^{\circ}\mathrm{C}$. This must be related to the particular microstructure of film 4, which consists in a dense matrix (with relatively low H content incorporated as isolated monohydride groups) containing small isolated voids at the surface of which polyhydride complexes and interacting Si-H groups are located, as previously suggested,[27] rather than in an ''island and tissue'' type matrix.[28] Moreover, the optoelectronic properties of film 2, deposited under nonoptimized conditions, can be improved by a simple annealing of the native defects at $T_A = 250\,^{\circ}\mathrm{C}$. We may add that the standard films 2 and the He-diluted films 4 deposited under completely different plasma conditions (Table I) seem to exhibit in the as-deposited state similar modes of H incorporation despite the differences in their microstructure and their total bonded hydrogen content. On the contrary, the He-diluted films 4 deposited at high rate present in the as-deposited state optoelectronic properties (N_D, E_0, and N_S) very similar to those of the optimized standard films 3 deposited at low rate at the same T_S.

IV. CONCLUSION

By the present annealing studies on a-Si:H samples prepared under different plasma and substrate temperature conditions, we have evidenced the difference in the H bonding modes between the He-diluted films deposited at high rates and the standard samples deposited at low rates. We observe higher H stability with respect to the annealing temperature in the former case, i.e., in these films the total bonded H content starts to decrease at higher T_A. The defect creation processes depend strongly on both the film microstructure and the hydrogen bonding configurations, particularly the isolated monohydride content initially present in the samples. The high-temperature annealing (departure of H) creates less defects in the optimized He-diluted samples than in optimized standard samples deposited at the same (high) T_S (250 °C). We also demonstrate that despite a higher total bonded H concentration, with a relatively large proportion of Si-H in cavities (2080-cm^{-1} stretching band) and possibly a small proportion of polyhydride groups (840-cm^{-1} bending band), the He-diluted samples in their as-deposited state show a very low defect density as well as a low disorder parameter, comparable to those obtained for the optimized standard films deposited at the same substrate temperature. Consequently, the He-diluted plasma conditions yield an interesting alternative method for fast deposition of a good quality material. Finally, for some standard samples deposited under nonoptimized conditions, we can significantly improve the optoelectronic properties of these films by annealing at 250 °C, i.e., well below the temperature of H release from the different hydrogen bonds.

*Permanent address: Laboratoire d'Optique des Couches Minces, Institut de Physique, Université d'Oran-es-sénia, Oran, Algeria.

†Permanent address: Department of Physics, PdF Masaryk University, 60300 Brno, Czech Republic.

[1] See, for example, *Semiconductors and Semimetals*, edited by P. K. Willardson and A. C. Beer (Academic, New York, 1984), Vol. 21.

[2] See, for example, I. Solomon, in *Amorphous Semiconductors*, edited by M. H. Brodsky, Topics in Applied Physics Vol. 36 (Springer-Verlag, Berlin, 1979); L. Ley, in *Physics of Hydrogenated Amorphous Silicon II*, edited by J. D. Joanopoulos and G. Lucovsky, Topics in Applied Physics Vol. 56 (Springer-Verlag, Berlin, 1984).

[3] J. C. Knights and R. A. Liyan, Appl. Phys. Lett. **35**, 244 (1979).

[4] G. Lucovsky, B. N. Davidson, G. N. Parsons, and C. Wang, J. Non-Cryst. Solids **144**, 154 (1989).

[5] P. Roca i Cabarrocas, J. B. Chévrier, J. Huc, A. Lloret, J. Y. Parey, and J. P. M. Schmitt, J. Vac. Sci. Technol. A **9**, 2331 (1991).

[6] P. Roca i Cabarrocas, R. Vanderhagen, Y. Bouizem, M. L. Thèye, D. Mencaraglia, Z. Djebbour, J. Sib, J. P. Kleider, C. Longeaud, and C. Godet, in *Proceedings of the 10th European Communities Photovoltaic Solar Energy Conference*, edited by A. Luque, G. Sola, W. Palz, G. Dos Santos, and P. Helm (Kluwer Academic, Dordrecht, 1991), p. 1083.

[7] R. Roca i Cabarrocas, Y. Bouizem, and M. L. Thèye, Philos. Mag. B **65**, 1025 (1992).

[8] P. Roca i Cabarrocas, Z. Djebbour, J. P. Kleider, C. Longeaud, D. Mencaraglia, J. Sib, Y. Bouizem, M. L. Thèye, J. Sardin, and J. P. Stoquert, J. Phys. (France) I **2**, 1979 (1992).

[9] R. Meaudre, M. Meaudre, P. Roca i Cabarrocas, S. Tanidi, Y.

Bouizem, and M. L. Thèye, J. Non-Cryst. Solids **137-138**, 171 (1991).
[10] K. Zellama, J. H. von Bardeleben, V. Quillet, Y. Bouizem, P. Sládek, M. L. Thèye, and P. Roca i Cabarrocas, J. Non-Cryst. Solids **164-166**, 285 (1993).
[11] A. A. Langford, M. L. Fleet, B. P. Nelson, W. A. Lanford, and N. Maley, Phys. Rev. B **45**, 13 367 (1992).
[12] P. Sládek, Y. Bouizem, M. L. Thèye, and P. Roca i Cabarrocas, in *Proceedings of the 11th European Communities Photovoltaic Solar Energy Conference*, edited by L. Guimaraes, W. Palz, C. De Reyff, H. Keiss, and P. Helm (Harwood Academic, Geneva, 1993), p. 710.
[13] P. Roca i Cabarrocas, J. Non-Cryst. Solids **164-166**, 37 (1993).
[14] H. Shirai, B. Drevillon, N. Layadi, and P. Roca i Cabarrocas, J. Non-Cryst. Solids **164-166**, 119 (1993).
[15] S. J. Jones, Y. Chen, D. L. Williamson, U. Kroll, and P. Roca i Cabarrocas, J. Non-Cryst. Solids **164-166**, 131 (1993).
[16] S. M. Myers, D. M. Bishop, D. M. Follstaedt, H. J. Stein, and W. R. Wampler, in *Microcrystalline Semiconductors: Materials Science and Devices*, edited by P. M. Fauchet *et al.*, MRS Symposia Proceedings Vol. 283 (Materials Research Society, Pittsburgh, 1993), p. 549.
[17] G. Sardin and J. L. Morenza, Solar Energy Materials **20**, 189 (1990). See also related references inside.
[18] W. Beyer and H. Wagner, J. Phys. (Paris) Colloq. **42**, C4-783 (1981).
[19] L. Chahed, M. L. Thèye, and B. Bourdon, J. Phys. **44**, 387 (1983).
[20] K. Zellama, P. Germain, S. Squelard, J. M. Berger, F. Dechelle, J. P. Ferraton, A. Donnadieu, and B. Bourdon, Solid State Commun. **56**, 721 (1985).
[21] D. Jousse, E. Bustaret, and F. Boullitrop, Solid State Commun. **55**, 485 (1985).
[22] S. K. Deb, Thin Solid Films **163**, 75 (1988).
[23] J. P. Kleider, C. Longeaud, and P. Roca i Cabarocas, J. Non-Cryst. Solids **164-166**, 403 (1993).
[24] D. K. Biegelsen, R. A. Street, C. C. Tsai, and J. C. Knights, Phys. Rev. B **20**, 4839 (1979).
[25] M. Stutzmann, Philos. Mag. B **60**, 531 (1989).
[26] D. Adler, Solar Cells **9**, 133 (1983).
[27] H. Wagner and W. Beyer, Solid State Commun. **48**, 585 (1983).
[28] W. Paul, in *Amorphous Silicon and Related Materials Vol. 1A*, edited by H. Fritsche (World Scientific, Singapore, 1988), p. 63.